Novel Passive Discrete Variable Stiffness Joint (pDVSJ): Modeling, Design, and Characterization

Mohammad I. Awad*[1]. *IEEE Student Member*, Dongming Gan[1], Ali Az-zu'bi[1], Jaideep Thattamparambil[1], Cesare Stefanini[1], Jorge Dias[1,2] *IEEE Senior Member* , Lakmal Seneviratne[1,3]

***Abstract*— In this paper, the design and characterization of a novel passive Discrete Variable Stiffness Joint (pDVSJ) is presented. The pDVSJ is a proof of concept of a passive revolute joint with discretely controlled variable stiffness. The current realization is equipped on a passive single-DOF exoskeleton (TELEXOS-I) for future development towards applications in haptic-teleoperation purposed exoskeletons. The key motivation behind this design is the need of instantaneous switching between stiffness levels when applied for Virtual Reality (VR) or Remote Environment (RE) stiffness mapping applications, in addition to the need of low-energy-consumption. Altering the stiffness is achieved by selecting the effective length of an elastic rubber cord. This is realized by creating a new grounding point, thus changing the effective length. Three different levels of stiffness (low, moderate, high) can be discretely selected beside the zero stiffness. The novelty of this work lies in the method used to alter the stiffness of the variable stiffness joint, and the design of Cord Grounding Units (CGUs) which are responsible for selecting the effective length of the elastic cord. The main features of CGU are the fast response and the low-energy consumption. This is achieved through a linear solenoid actuator pushing a cam-cleat which will clutch the motion of the elastic cord, creating a new grounding point. This will limit the length of the cord between the cam cleat and the cord's fitting point on the joint. The solenoid's ON-Time is minimized as the cam cleat's design is passively self-locking the cord through the pulling force between the cord and the cam-cleat. The proposed physical-based model matched the experimental results of the pDVSJ in terms of discrete stiffness variation curves and the stiffness dependency on the behavior of the elastic rubber cord.**

I. INTRODUCTION

In the last decades, the world witnessed a significant boost in the development of haptic interfaces which enhanced their capabilities in conveying information of remote or virtual environment. This information is conveyed to the operator through touch, force or torque [1]. Haptic interfaces is currently applied in several applications and many fields such as tele-navigation [2-5], tele-rehabilitation [6, 7], tele-surgery [8. 9] and micro-manipulation [10, 11].

Based on their haptic stimuli actuation system, haptic interfaces are classified into active, passive and hybrid. Active haptic interfaces are equipped with actuators that can add or dissipate energy from the system such as motors. Active haptic interfaces have been widely presented in literature, some are grounded like the famous PHANTOM [12], arm exoskeletons [13], and some are wearable like the haptic gloves [14, 15]. On the other hand, passive haptic interfaces are devices that incorporate energetically passive actuators in order to remove, store or redirect kinetic energy within the system [16]. Energy dissipative haptic devices are intrinsically safe and stable compared to their active counterparts, but they're unable to restore energy [17]. Lastly, the hybrid haptic devices apply both active and passive actuation in order to gain the safety and stability of passive actuators and the ability to perform energy restitution from the active actuators [17]. Passive and hybrid haptic interfaces incorporate several types of energy dissipative passive actuators such as electromagnetic dry friction clutches [18], electro-rheological (ER) clutches [19], programmable differential breaks [21], Eddy Current Breaks [22].

Elastic elements were also introduced to haptic device's actuation systems. An example is applying the elastic cords for obtaining egocentric haptic feedback through a body-mounted elastic armature (Elastic Arm) [24]. On the same hand, fabric's stiffness was involved in haptic devices such as the Bi-elastic fabric softness display [25]. Recently, haptic interfaces were incorporated with serial elastic actuators (SEA) to enhance the closed loop behavior and reduce the output impedance [23]. The drawbacks of the SEA lie in the non-optimal performance and non-optimal energy efficiency. The optimal performance needs careful tuning of the joint stiffness values [26, 27]. This motivated lots of study and new designs of variable stiffness mechanisms with passive compliance for haptic applications such as the pVSJ [27].

An evolution of variable stiffness actuators (VSA) is the antagonistic variable stiffness actuators, where the joint stiffness is varied through the combination of two antagonistic SEAs controlled by two separate motors. Designs which fall into this category include VSA-I [28], VSA-II [3329]. This type lacks energy efficiency as it requires two motors to adjust the stiffness. In order to overcome this problem several solutions such as altering the link length between the pivot and either the elastic element or the output link. Examples of this type include the AwAS

Mohammad I. Awad is corresponding author (mohammad.awad@kustar.ac.ae)

[1] Authors are with the Khalifa University Robotics Institute, Khalifa University of Science Technology and Research, Abu Dhabi, United Arab Emirates

[2]Authors are with Institute of Systems and Robotics and the Faculty of Science and Technology, University of Coimbra, Coimbra, Portugal

[3]Authors are with King's Collage London, UK

[3630], AwAS-II [31], CompAct-VSA [32]. On the same hand, an energy-efficient solution can be realized through discretely selecting the stiffness of the VSA by changing the engagement of elastic material discretely using low power electro-adhesive clutches [33].

In this paper, a new passive variable stiffness joint is presented, the proof of concept shows the ability of the joint of switching between levels of stiffness in very short time and minimized energy consumption. The concept and the mechanical design are presented in section II. The elastic cord behavior and the system physical model are presented in section III. The system's implementation and the model verification is done in section IV. In section V, a discussion for research guidance and future enhancements is illustrated. Finally, in section VI, the conclusions and the intended future work are presented.

II. Concept & Mechanical Design

A. pDVSJ Concept and Functionality

In order to achieve the purpose of teleoperation with stiffness mapping of remote (or virtual) environment, a haptic interface should bare many features such as (1) maintaining transparency (zero stiffness) while no virtual feature is being touched, (2) the transition between one level of stiffness and the other should be instantaneous to insure better mapping quality, (3) the stiffness engagement should occur at any degree of joint deflection and (4) low energy consumption. The idea of the passive Discrete Variable Stiffness Joint (pDVSJ) is driven by these requirements.

The concept of pDVSJ is inspired from the antagonistic variable stiffness actuators (VSA). The stiffness of the joint is altered instantaneously by discretely selecting the effective length of an elastic cord. The basic concept is shown in (fig. 1). An elastic rubber cord with a total length of (L_{tot}) is grounded from one side and an output force (F) on the other side is generated subjected to an elongation (Δx). It is well known that the stiffness of an elastic cord is inversely related with its length. Thus by engaging different length of the elastic cord in the system, the effective stiffness can be varied. In the pDVSJ, a new grounding point (G) is created by clutching the cord at that particular point creating instantaneously a new active length (L_j). Before the engagement, the output force is $F = \Delta x * k_1$, and it is $F = \Delta x * k_2$ for the same elongation after the engagement with the effective length L_j. Applying this approach in altering the stiffness of the elastic material in variable stiffness joints is believed by the authors to be novel.

The pDVSJ (shown in fig. 2) consists of an elastic cord mounted on two pulleys. The cord is fixed on two symmetrical points (Points A, A*) on the joint pulley while winds around the driven pulley. A set of six Cord Grounding Units (CGU) allow the cord to move freely while not activated, resulting in transparency (zero stiffness value). A CGU will prevent the cord from moving in one direction if activated to create a grounding point, the position of the grounding point will define the effective length of the involved elastic cord. The CGUs labeled (L, M, H) are assigned to prevent the cord of moving in the direction when the output link is moving Counter Clockwise (CCW) while the CGUs labeled (L*, M*, H*) will prevent Clockwise (CW) motion. The labeling (L, M, H) is referred to Low, Moderate and High levels of stiffness respectively. The (*) refers for any entity or variable that is related for the CW motion.

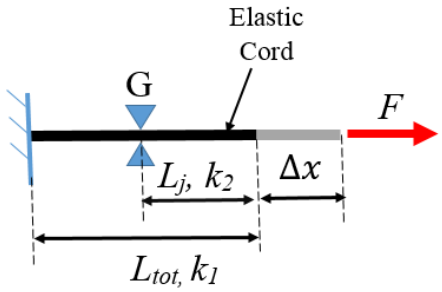

Figure 1: Basic Concept of pDVSJ

Minimizing the energy consumption is the core-feature of the CGU design. Each CGU is pulse controlled and requires only a 1-second pulse to be activated. An activated CGU keeps holding the cord as long as it is moving in the intended direction and will release the cord passively when a flip in the motion is experienced.

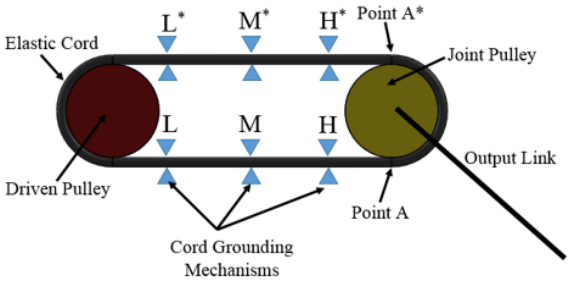

Figure 2. Functionality of pDVSJ

B. Cord Grounding Unit

The Cord Grounding Unit (CGU) is a key component in the pDVSJ. It is responsible for creating the grounding point through clutching the motion of the elastic cord on a defined position in order to alter the stiffness of the joint. The CAD model of the CGU is shown in (fig. 3). The CGU is composed of a frame, a cam-cleat, a linear solenoid actuator, and a leaf spring. The cam-cleat's shaft is mounted on the frame and can rotate freely. Unlike the regular cam-cleat applications, the leaf spring is responsible of retracting the cam-cleat away from the clinging point. The linear solenoid actuator is responsible to push the cam cleat towards the moving cord in the case when it is required to alter the stiffness of the joint (see fig. 4a). The cam-cleat design aims to eliminate the space between the cord and the frame. If the cord is moving towards the direction where it can pull the cam-cleat towards clinging point (yellow arrow) (see fig. 4b), the cam cleat utilizes the pulling force from the moving cord and maintains a passive push force on the cord (see fig. 4c). This force will clutch the cord's motion in one direction and maintain clutching until a flip in the motion direction occurs. When the motion direction flips, disengagement occurs and the leaf spring will retract the cam cleat to its initial position.

The key feature of the CGU is its low energy-consumption. Activating the solenoid is only required to maintain a "touch" between the cam-cleat and the cord before the cord start pulling the cam cleat. In identical scenario, where the cord's

motion is not affected significantly by its elasticity along its length, the ON-time of the linear solenoid actuator will be a short period of time (i.e. one second) and it's directly dependent on the cord's axial velocity. As higher axial velocity of the cord will reflect in shorter time of reaching the clinging point of the cam cleat.

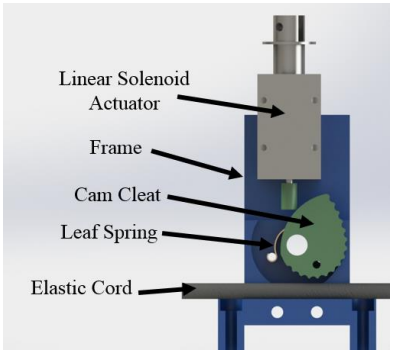

Figure 3: Anatomy of Cord Grounding Unit

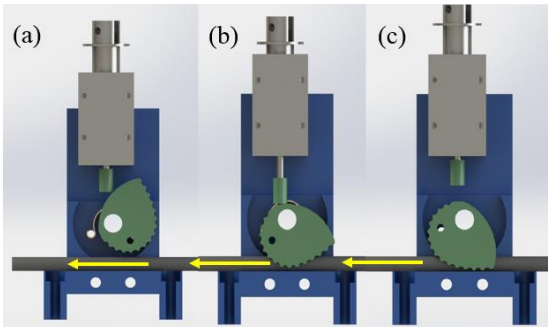

Figure 4: Cord Grounding Unit Operating Stages

C. pDVSJ equipped on TELEXOS-I

The pDVSJ is mounted on a light weight, passive single DOF wearable elbow exoskeleton (TELEXOS-I) (see fig. 5) which is purposed for haptic teleoperation. TELEXOS-I is equipped with an optical encoder for measuring the joint deflection, and Force/Torque sensor for measuring the external torque on the elbow. The user will wear the system on their right-arm to perform haptic teleoperation missions. The system is aimed to map stiffness from Virtual Reality (VR) or Remote Environment (RE). When the system receives a high level of mapped stiffness from VR or RE, the controller will activate either CGU-H or CGU-H* depending on the user's direction of motion (CCW or CW respectively). Similarly, if the intended level of mapped stiffness is moderate the controller will activate either CGU M or CGU M* based on the joint motion. A low stiffness reflection can be also provided by activating CGU-L or CGU-L*.

III. Stiffness Modeling

A. Cable Stiffness Regions

The elastic element in the pDVSJ is an elastic rubber cord. It is well known that rubber's elastic behavior does not follow Hook's Law as entropy effects significantly in its behavior [34]. This explains why stiffness of the rubber depends on several factors such as (1) Ambient Temperature, and (2) the rubber's cross link density [34]. Including these factors will add undesired complexity to the system's model. Due to these reasons, it is worthwhile to study the operating regions of the elastic cord in order to select a preferred region that can ease the stiffness modeling.

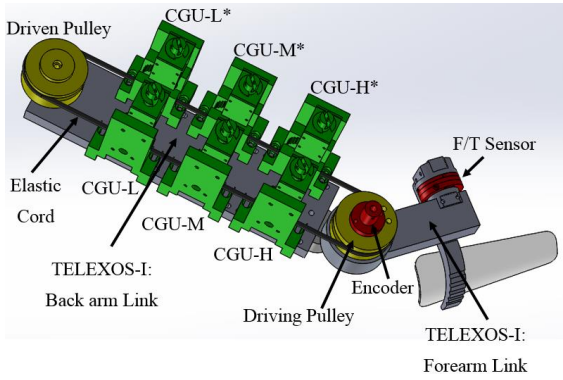

Figure 5: The pDVSJ equipped on TELEXOS-I

Three samples of the *Nike ® Long Length Resistance Band 2.0* with initial lengths, (69mm, 140mm, and 172mm) were tested on Tensile Test Machine (Instron 5969) and the results are shown in (fig. 6). The force vs. strain graph shows that cord behaves in a logarithmic behavior in the first region (strain: 0 to 0.1), then it behaves linearly on the second region (strain: 0.1 to 1.15), and then it changes to higher power orders in the third region (strain: 1.15 to 1.4). Therefore, the desired operating region of this cord is chosen to be the linear region. For that, a minimum pretention of 0.1 strain should be set.

From Fig. 6, the stiffness of the elastic cord (k_j) in the linear region can be determined if the free length (L_{j0}) of the cord is known through ($k_j = \frac{K}{L_{j0}}$) Where K is the rate of change in load force with respect to strain obtained (K=62.1 N) from Fig.6.

B. Stiffness Modeling of the pDVSJ

In the pDVSJ, the stiffness is altered through altering the effective length of an elastic rubber cord. Fig. 7 shows that the effective length can be selected through activating the desired CGU's and is measured from the fitting points (A, or A*) to the active CGU. If the intended stiffness value is high, moderate or low then the effective length will be L_H, L_M or L_L respectively. Sufficient pretention (26% of the free length) is added to move to the linear region and minimize the slippage when mounting the cord onto the two pulleys.

A stiffness model of the joint is presented in this section. It is assumed that the joint will operate in room temperature, and the rubber cord cross link density will not be effected by the cross-sectional compression applied from the CGU. It is also assumed that the cord with the active length and the cord with the remaining length behave independently from each other.

The total length of the mounted cord can be calculated through ($L_{tot} = L_0 + p_{tot}$) where L_0, p_{tot}, are the un-stretched rubber cord length (free length), and the total

pretention respectively. If the direction of motion is counter-clockwise, the effective lengths (L_H , L_M or L_L) are measured from point A to points H, M, or L respectively. And they are measured from A* to H*, M*, or L* respectively in the clockwise case. The remaining length ($\widetilde{L_\iota}$) can be directly calculated through ($\widetilde{L_\iota} = L_{tot} - L_i \, , i \in \{H, M, L\}$), The un-stretched effective length (L_{i0}) and the remaining un-stretched length ($\widetilde{L_{\iota 0}}$) can be obtained by ($L_{i0} = \left(\frac{L_0}{L_{tot}}\right) L_i$, $\widetilde{L_{\iota 0}} = \left(\frac{L_0}{L_{tot}}\right) \widetilde{L_\iota}$, $i \in \{H, M, L\}$). In order to get the value of the effective pretention (p_i) and the remaining pretention ($\widetilde{p_\iota}$), the following formulas are applied ($p_i = \left(\frac{L_{tot} - L_0}{L_{tot}}\right) L_i$, $\widetilde{p_\iota} = \left(\frac{L_{tot} - L_0}{L_{tot}}\right) \widetilde{L_\iota}$) $i \in \{H, M, L\}$).

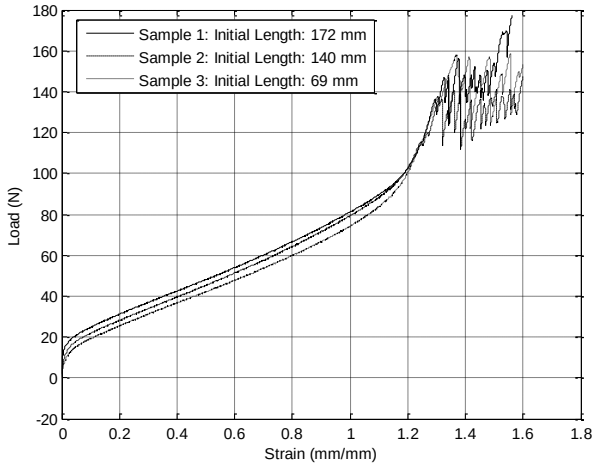

Figure 6: Load versus Strain for *Nike ® Long Length Resistance Band 2.0*

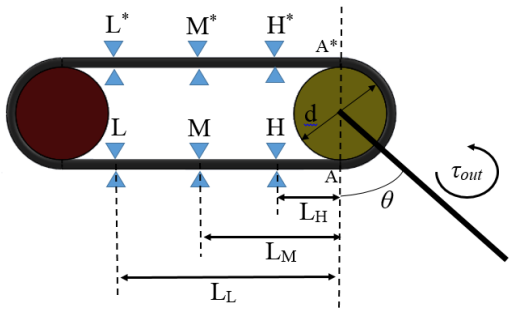

Figure 7. Model of the pDVSJ

The output torque (τ_{out}) formula can be written as following:

$$\tau_{out} = \frac{d}{2}\left(k_i \Delta x_i - \widetilde{k_\iota} \Delta \widetilde{x_\iota}\right) \qquad i \in \{H, M, L\} \qquad (1)$$

$$\Delta x_i = p_i + \frac{d}{2}\Delta\theta \qquad i \in \{H, M, L\} \qquad (2)$$

$$\Delta \widetilde{x_\iota} = \widetilde{p_\iota} - \frac{d}{2}\Delta\theta \qquad i \in \{H, M, L\} \qquad (3)$$

where k_i,$\widetilde{k_\iota}$, d, θ are the cord's stiffness of the effective length, cord's stiffness of the remaining length in the linear region, the pulley's diameter, and the joint's deflection respectively. Substituting equations (2 and 3) into equation (1), then deriving with respect of the joint's angular position (θ). The joint's stiffness (K_θ) can be derived as following:

$$K_\theta = \frac{\partial \tau_{out}}{\partial \theta} = \left(\frac{d}{2}\right)^2 \left(\frac{K}{L_{i0}} + \frac{K}{\widetilde{L_{\iota 0}}}\right) \qquad i \in \{H, M, L\} \qquad (4)$$

From equation (4), it is shown that the joint's stiffness can be discretely chosen by selecting the effective length.

IV. Implementation and Validation of the PDVSJ

TELEXOS-I consists of two Teflon links that can be strapped to the user arm. The back arm is (275 mm) long and consists of a link, a base for the CGU's and the driven pulleys. The forearm link is (112.5 mm) and has a base of the force/torque sensor at (100 mm). In order to ensure compliance of the contact between the exoskeleton and the user's arm, TELEXOS-I is equipped with shin pads and soft nylon contacts. The pulleys (driver and driven) are made of Aluminum Alloy with (55 mm) diameter. The elastic cord (*Nike ® Long Length Resistance Band 2.0*) has a total of free length of (575 mm). Pretention of (155 mm) is added to the cord to obtain a strain of (0.27) before fitting the cord into the driver pulley. The cam-cleats and the frames of the six Cord Grounding Units (CGU) were 3D printed and are made of ABS Light Plastic. The CGUs were mounted along the base on the back arm so that the effective lengths will be L_H=60 mm, L_M= 128 mm and L_L= 196 mm. The Linear Solenoid Actuators operate at 24 VDC and draw a current of 1.7 Amperes each while active. The system's design parameters are illustrated in table 1.

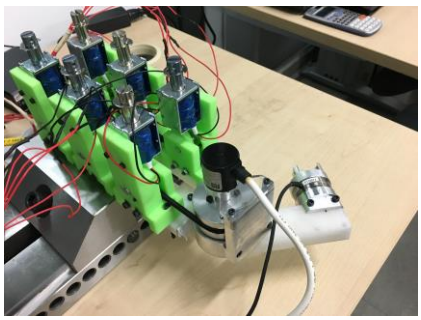

Figure 8. Charactrization expirement of pDVSJ with TELEXOS-I

The sensory of TELEXOS-I consists of a force/torque sensor (ATI Mini 40) mounted on the forearm, and a quadrature rotary encoder (RS-260-3768) mounted on the driver pulley. A National Instrument DAQ (NI-USB-6343) and the National Instrument LabVIEW® were used for real time control and data acquisition. The test for characterization was performed on a horizontal vice (fig. 8) to eliminate any effect of gravitational potential energy, and without the shin pads in order to eliminate the effects of any elastic potential energy from external entities in order to have a clear model validation.

The theoretical levels of stiffness based on the system's parameters are shown in Table 2. In order to verify the model,

several experiments were conducted. By selecting to activate the desired CGU, the user will apply the external torque through a block held by their hand in order to deflect the joint from the home position (zero degrees) to around 90 degrees. The deflection was measured by the optical encoder and the external torque was measured by the force/torque sensor.

In (fig. 9), the experimental results (black circles) have validated the presented theoretical model (red lines) for all the three stiffness levels. It's worth to mention that at deflection (1.4 rad) for high stiffness (CGU-H), the strain of the cord was (1.13), which indicates that the cord has switched to third region of behavior, which adds another validation for the presented cord model.

Regarding the system's energy consumption, it is noted that the solenoid's ON-time under a joint average angular speed of (5.2 degrees/s) is (1 second). It's also worth to mention that due to the friction between the driven pulley and its base, the elasticity of the cord has significantly affected behavior of the cord's motion flow "pull-stretch-pull". A change in the position of the joint's link will immediately change the position of the cord that is near to the joint pulley. For long active lengths, the cord's body will stretch till the accumulated elastic energy is sufficient to overcome friction force and move the driven pulley. This will require the solenoids of CGU-M and CGU-L to stay on for more time (2, and 3 seconds respectively) compared to CGU-H. The system's power, and physical specifications are shown in Table 3.

TABLE I. PDVSJ DESIGN PARAMERTERS & SPECIFICATIONS

Specification	Value	Unit
Cord's stiffness per unit length (K)	62.1	N
TELEXOS-I Back Arm Length	0.27	m
TELEXOS-I Forearm Link Length	0.12	m
Pulley's Diameter	0.055	m
Elastic Cord Free Length	0.575	m
Total Pretention of Cord	0.155	m
Cords effective Length from CGU-H (L_H)	0.06	m
Cords effective Length from CGU-H (L_M)	0.128	m
Cords effective Length from CGU-H (L_L)	0.196	m

TABLE II. THEORTICAL RESULTS BASED ON SYSTEM'S PARAMETERS

High Stiffness (N.m/rad)	Moderate Stiffness (N.m/rad)	Low Stiffness (N.m/rad)
1.08	**0.56**	**0.41**

TABLE III. SYSTEM'S POWER AND PHYSICAL SPECFICATIONS

Specification	Value	Unit
Operating Voltage	24	VDC
Operating Current	1.7	A
Power Consumption for Single CGU	40.8	W
Maximum Energy Consumption to alter a level of stiffness	122.4	J
Minimum Energy Consumption to alter a level of stiffness	40.8	J
Linear Solenoid Actuator response time	40	ms
Single CGU Mass	225	g
Single Linear Solenoid Actuator	150	g
TELEOX-I mass (without PDVSJ)	1170	g
System's Gross Mass	2642	g

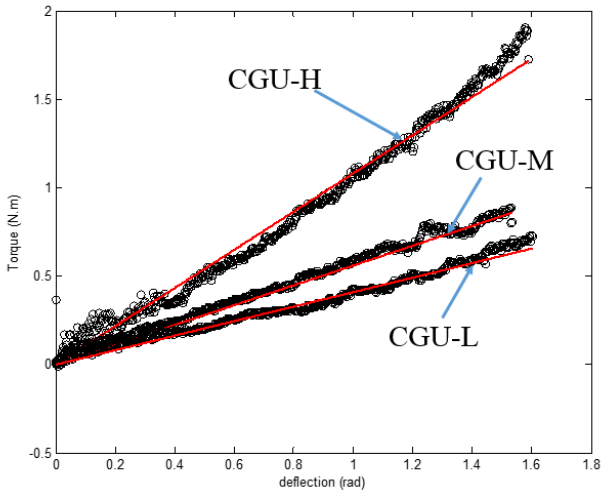

Figure 9 : Joint's Torque versus deflection :Theoretical results (Red Lines), expiremental results (black circles)

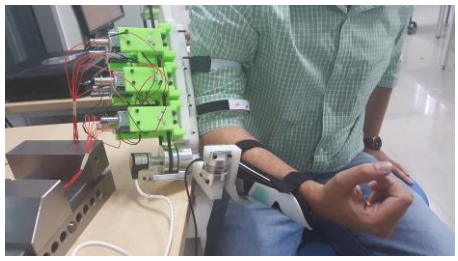

Figure. 10 Realization of pDVSJ with TELEXOS-I

In order to get higher levels of stiffness, a "stronger" elastic cord could be used. This can be realized by either using a thicker cord or changing the cord's material. Selecting a thicker cord will add more clinging time for the cam cleat as they will need more deformation to reach the clinging point. The authors recommend to obtain a rubber material that shows (1) high stiffness, (2) short length recovery time, and (3) low cross-sectional area.

The main contributor to the system's mass is the linear solenoid actuators (150 g/actuators). A significant reduction of the mass can be achieved by selecting smaller solenoids as low output solenoid force is sufficient.

V. CONCLUSION

In this paper, the mechanical design, physical model and system characterization of the novel passive Discreet Variable Stiffness Joint (pDVSJ) were presented. The joint's stiffness is altered discretely through selecting the effective length of the elastic rubber cord. This method used to realize the concept is novel. Altering the stiffness is realized through activating one of the novel Cord Grounding Units, which is responsible for clutching the cord's motion, creating a new grounding point, thus limiting its effective length.

A study of the cord's behavior was conducted and the stiffness properties of the cord was applied to model the joint stiffness. To have a clear model, pretention was used to make the pDVSJ operate only in the linear region of the cord. This

was achieved through adding pretention to the cord to avoid operating in the first region and by selecting the maximum elongation to be below the third region. The physical model was presented and verified through experimental results, which showed that the joint is capable of switching to the three levels of stiffness. The energy-consumption is minimized as a result of the novel design of the Cord Grounding Unit which only requires short ON-Time for the actuator as the system is self-locking.

In the future, a more compact and light-weight design underlying on identical concept will be realized, but focusing on attaining more levels of stiffness, and less numbers of actuators. The authors intend to investigate the nonlinear regions of the cord's behavior and their effects on the stiffness performance.

REFERENCES

[1] Hayward, O. Astley, M. Cruz-Hernandez, D. Grant, and G. Robles-De-La-Torre, "Haptic interfaces and devices," Sensor Rev., vol. 24, pp. 16–29, Nov. 2004.

[2] S. Lee, G. S. Sukhatme, G. J. Kim, and C.-M. Park, "Haptic control of a mobile robot: A user study," presented at the IEEE/RSJ Int. Conf. Intelligent Robots and Systems, Lausanne, Switzerland, Oct. 2002.

[3] S. K. Cho, H. Z. Jin, J. Lee, and B. Yao, "Teleoperation of a mobile robot using a force-reflection joystick with sensing mechanism of rotating magnetic field," IEEE/ASME Trans. Mechatronics, vol. 15, no. 1, pp. 17– 26, Feb. 2010.

[4] L. M. Crespo and D. J. Reinkensmeyer, "Haptic guidance can enhance motor learning of a steering task," J. Motor Behavior, vol. 40, no. 6, pp. 545–556, 2008.

[5] X. Chen and S. Agrawal, "Assisting versus repelling force-feedback for learning of a line following task in a wheelchair," IEEE Trans. NeuralSyst. Rehabil. Eng., vol. 21, no. 6, pp. 959–968, Nov. 2013.

[6] T. Coles, D.Melange, and N. John, "The role of haptic in medical training simulators: A survey of the state of the art," *IEEE Trans. Haptics*, vol. 4, no. 1, pp. 51–66, Jan./Feb. 2011.

[7] M. Ferre, I. Galiana, R. Wirz, and N. Tuttle, "Haptic device for capturing and simulating hand manipulation rehabilitation," *IEEE/ASME Trans. Mechatronics*, vol. 16, no. 5, pp. 808–815, Oct. 2011.

[8] F. Gosselin, C. Bidard, and J. Brisset, "Design of a high fidelity haptic device for telesurgery," in *Proc. IEEE Int. Conf. Robot. Autom.*, Apr. 18–22, 2005, pp. 205–210.

[9] X. Wang and P. X. Liu, "Improvement of haptic feedback fidelity for telesurgical applications," *Electron. Lett.*, vol. 42, no. 6, pp. 327–329, 2006.

[10] Z. Ni, A. Bolopion, J. Agnus, R. Benosman, and S. Regnier, "Asynchronous event-based visual shape tracking for stable haptic feedback in microrobotics," *IEEE Trans. Robot.*, vol. 28, no. 5, pp. 1081–1089, Oct. 2012.

[11] Bolopion and S. Regnier, "A review of haptic feedback teleoperation systems for micromanipulation and microassembly," *IEEE Trans. Autom. Sci. Eng.*, vol. 10, no. 3, pp. 496–502, Jul. 2013.

[12] J.K. Salisbury and M.A. Srinivasan, Proc." First Phantom Users Group Workshop", 1996

[13] A. Gupta and M. K. O'Malley. Design of a haptic arm exoskeleton for training and rehabilitation. Trans. Mechatronics, 11(3):280–289, 2006.

[14] M. Turner, D. Gomez, M. Tremblay, and M. Cutkosky, "Preliminary tests of an arm-grounded haptic feedback device in telemanipulation," in Proc. ASME Dyn. Syst. Control Div., 1998, vol. DSC-64, pp. 145–149.

[15] Zhou MA, Pinhas Ben-Tzvi, "RML Glove—An Exoskeleton Glove Mechanism With Haptics Feedback", IEEE/ASME Transaction on Mechatronics, VOL. 20, NO. 2, April 2015, pp. 641-652

[16] D. K. Swanson. Implementation of Arbitrary Path Constraints using Dissipative Passive Haptic Displays. PhD thesis, School of Mechanical Engineering, Georgia Institute of Technology,, 2002.

[17] Carlos Rossa, Jos_e Lozada, and Alain Micaelli, "Design and Control of a Dual Unidirectional Brake Hybrid Actuation System for Haptic Devices" IEEE Transaction on Haptics, VOL. 7, NO. 4, 2014, pp. 442-453

[18] W. J. Book, R. Charles, H. Davis, M. Gomes, and K. Danai, "The concept and implementation of a passive trajectory enhancing robot," in Proceedings of the ASME Dynamic Systems and Control Division, Atlanta, GA, pp. 633{638, 1996.

[19] M. Sakaguchi and J. Furusho, \Development of a 2 DOF force display system using ER actuators," in IEEE/ASME Conference on Advanced Intelligent Mechatronics, Atlanta, GA, pp. 707{712, 1999.

[20] Yaroslav Tenzer _, Brian L. Davies, Ferdinando Rodriguez y Baena," Programmable differential brake for passive haptics", Robotics and Autonomous Systems 58 (2010) 249_255

[21] Andrew H. C. Gosline, and Vincent Hayward, Eddy Current Brakes for Haptic Interfaces: Design, Identification, and Control, IEEE/ASME TRANSACTIONS ON MECHATRONICS, VOL. 13, NO. 6, DECEMBER 2008, pp. 669-677

[22] Yun-Joo Nam and Myeong-Kwan Park, "A Hybrid Haptic Device for Wide-Ranged Force Reflection and Improved Transparency, International Conference on Control, Automation and Systems 2007, pp. 1015-1020

[23] E. Basafa, M. Sheikholeslami, A. Mirbagheri, F. Farahmand, G. R. Vossoughi, "Design and Implementation of Series Elastic Actuators for a Haptic Laparoscopic Device", Annual International Conference of the IEEE EMBS, 2009, pp. 6054-6057.

[24] Merwan Achibet et al. Elastic-Arm: Human-scale passive haptic feedback for augmenting interaction and perception in virtual environments, IEEE conference of Virtual Reality (VR), 2015, pp. 63 - 68

[25] M. Bianchi, E. P. Scilingo, A. Serio, A. Bicchi, "new softness display based on bi-elastic fabric, Third Joint Eurohaptics Conference and Symposium on Haptic Interfaces for Virtual Environment and Teleoperator Systems, 2009. Pp. 382 - 393

[26] D. Gan, N. G. Tsagarakis, J. Dai, D. Caldwell, L. Seneviratne, Stiffness Design for a Spatial Three Degrees of Freedom Serial Compliant Manipulator Based on Impact Configuration Decomposition, Journal of Mechanisms and Robotics, 2013

[27] M. I. Awad et al. ," Modeling, Design & Characterization of A Novel Passive Variable Stiffness Joint (pVSJ)", in preceding in IEEE IROS 2016.

[28] Tonietti, G., Schiavi, R., and Bicchi, A, "Design and Control of a Variable Stiffness Actuator for Safe and Fast Physical Human/Robot Interaction," International Conference on Robotics and Automation, 2005,

[29] Jonathan W. Hurst , Joel E. Chestnutt ; Alfred A. Rizzi, "The Actuator With Mechanically Adjustable Series Compliance", IEEE Transactions on Robotics (Volume:26 , Issue: 4), 2010, pp. 597 – 606.

[30] A. Jafari, N. Tsagarakis, B. Vanderborght, and darwin Caldwell, "Awas: a novel actuator with adjustable stiffness," is in the Proceeding of IEEE/RSJ International Conference on Intelligent Robots and Systems (IROS), 2010.

[31] Amir Jafari, Nikos G. Tsagarakis and Darwin G. Caldwell. "AwAS-II: A New Actuator with Adjustable Stiffness based on the Novel Principle of Adaptable Pivot point and Variable Lever ratio" IEEE International Conference on Robotics and Automation, 2011, pp.4638-4643.

[32] N. G. Tsagarakis, I. Sardellitti, and D. G. Caldwell, "A new variable stiffness actuator (CompAct-VSA): Design and modelling," in Proc. IEEE/RSJ Int. Conf. Intell. Robots Syst., 2011, pp. 378–383.

[33] Stuart Diller , Carmel Majidi ; Steven H. Collins, "A lightweight, low-power electroadhesive clutch and spring for exoskeleton actuation", IEEE International Conference on Robotics and Automation (ICRA), 2016, pp. 682 - 689

[34] Treloar, Leslie Ronald George. "The physics of rubber elasticity". Oxford University Press, USA, 1975.